Adsorptive Removal of Pentavalent Arsenic from Aqueous Solutions by Granular Ferric Oxide

R. Zakhar,[a,*] J. Derco,[a] F. Čacho,[b] and O. Čižmárová[c]

[a]Department of Environmental Engineering, Faculty of Chemical and Food Technology, Slovak University of Technology in Bratislava, Radlinského 9, 812 37 Bratislava, Slovak Republic

[b]Institute of Analytical Chemistry, Faculty of Chemical and Food Technology, Slovak University of Technology in Bratislava, Radlinského 9, 812 37 Bratislava, Slovak Republic

[c]Thermo Fisher Scientific, Leškova 11, 811 04 Bratislava, Slovak Republic

doi: https://doi.org/10.15255/CABEQ.2021.2018

Original scientific paper
Received: October 1, 2021
Accepted: June 9, 2022

Arsenic contamination of water resources, which is characterized by strong carcinogenic and toxic impacts, is a global problem. Therefore, the present study is focused on the isotherm and kinetic studies of pentavalent arsenic As(V) adsorption with initial concentration of 1 000 μg L^{-1} from aqueous solutions onto granular ferric oxide (GFO). Adsorption experiments were carried out by batch method, and the equilibrium and kinetic data were evaluated by the Langmuir, Freundlich, Dubinin-Radushkevich, Redlich-Peterson and Sips isotherm model, and pseudo-first and pseudo-second order kinetic model. The results obtained from this study imply that the adsorption of As(V) onto GFO was favourable, physical and multilayer process. The Sips and Redlich-Peterson isotherm and the pseudo-first order kinetic model gave the best fit to experimental data according to the values of correlation coefficient. The maximum theoretical adsorption capacity from Langmuir isotherm model was determined to be 1 900 μg g^{-1}. In addition, the impact of different operating conditions such as As(V) initial concentration, adsorbent dose, agitation speed, pH, temperature, and presence of phosphates and silica on adsorption capacity of GFO was also investigated. As(V) was efficiently recovered from GFO by 0.1 M NaOH desorbing solution during the three adsorption-desorption cycles.

Keywords:
adsorption, arsenic, granular ferric oxide, isotherm models, kinetic models, regeneration

Introduction

The basic needs of mankind undoubtedly include access to quality and safe drinking water, which is a strategic raw material limiting the development of individual regions and entire geographical areas.[1] There are still many places in the world that not only suffer from water shortages, but also from its contamination with harmful and toxic substances. At present, arsenic contamination of water resources, which is characterized by strong carcinogenic and teratogenic impacts, is coming to the fore.[2]

Arsenic was characterized as the 20th most occurring trace element in the earth's crust, 14th in seawater, and 12th in the human body.[3] It is released into water bodies by natural weathering reactions, biological activity, geochemical reactions, volcanic emissions, and anthropogenic activities, including mining activities, fossil fuel combustion, use of arsenic-based pesticides, herbicides and crop desiccants, and use of arsenic additives to livestock feed.[4] From the water bodies it can be discharged in soils as well as sediments, and can be uptaken by plants. Plants such as rice, wheat, and oats can also absorb arsenic from the soil, which is irrigated with arsenic-contaminated water. Therefore, arsenic is often found in many crops. In addition, in some parts of the world arsenic-contaminated water is used for drinking purposes without treatment.[5]

In water, arsenic can be naturally found usually in two soluble arsenic forms such as As(III) (arsenite) and As(V) (arsenate).[6] The distribution of these two soluble forms in natural water mainly depends on the redox potential (ORP) and the pH of the water. Under oxidizing conditions, the predominant form is pentavalent arsenic (arsenate), which is present in arsenic acid (H_3AsO_4), and oxyanionic

*Corresponding author: E-mail: ronald.zakhar@stuba.sk

species such as $H_2AsO_4^-$, $HAsO_4^{2-}$ and AsO_4^{3-}.[7,8] Organic arsenic compounds such as monomethyl arseneous acid (MMA(III)), monomethyl arsenic acid (MMA(V)), dimethyl arseneous acid (DMA(III)), and dimethyl arsenic acid (DMA(V)) can also be naturally present in water. Usually, these compounds occur in water at a concentration less than 1 μg L^{-1} and due to this fact, they have no major significance in drinking water treatment.[9,10]

Arsenic contamination of water resources is a global problem, with reported studies in a large number of countries including Italy, Hungary, Serbia, Croatia, New Zealand, Bengal, Chile, Taiwan, Vietnam, Bangladesh, the United States, and Canada.[11,12] The concentration of arsenic in waters of the world varies considerably and can range from 0.5 to 5000 μg L^{-1}.[3]

Among the toxic and harmful pollutants, arsenic has high priority because it has been identified as a human carcinogen (Group 1), and can cause various chronic diseases. The toxicity and carcinogenicity of arsenic depends on its forms and oxidative states.[13] Many studies have indicated that arsenic ingestion can result in internal malignancies, including cancers of the kidney, bladder, liver, lungs, and other organs. It also has non-cancer effects that include cardiovascular, pulmonary, immunological, neurological, reproductive and endocrine (e.g. diabetes) disorders. In addition, arsenic has been shown to have genotoxicity. The health effects caused by acute arsenic poisoning are called arsenicosis, which has been also responsible for keratosis, skin changes and hyperkeratosis, skin lesions.[14–16] These aspects forced the World Health Organization (WHO) to reduce the maximum contaminant level of arsenic concentration in drinking water to 10 μg L^{-1} from earlier limit of 50 μg L^{-1} in 1993, which was also followed by the Unites States Environmental Protection Agency (US EPA) in 2001.[17]

Different technologies have been used and proposed to remove arsenic from aqueous media. Therefore, many different technologies can be found around the world. Adsorption has been universally accepted as one of the most effective arsenic removal processes because of its easy operation and handling, low cost, low consumption of reagents, and it does not produce sludge and harmful by-products.[3,10,18,19] Adsorption is the process of removing dissolved solids from solutions by accumulating them on a suitable interface, respectively on the solid phase surface. The adsorbed molecules (adsorbate) can be bound to the surface of the solid (adsorbent) by van der Waals forces (physical adsorption) or by chemical bonds (chemisorption).[19–22] When the adsorbent material has been exhausted, it must be regenerated in order to be reused again. Successful desorption is considered to obtain regenerated media with approximately equal initial adsorption properties as before.[23] The possibility of adsorbent regeneration is not discussed in most arsenic adsorption studies. Depending on the used adsorbent, temperature and flow rate of regenerating agent, the strongly acidic (HCl, H_2SO_4, HNO_3, H_3PO_4) or strongly basic eluents (NaOH) and neutral electrolytes (NaCl) can be used for regeneration of exhausted media.[24,25]

However, the desorption and regeneration process contributes to the accumulation of hazardous substances in concentrated form, which is related to the subsequent problem of safe disposal. Combustion is limited due to the volatility of arsenic-containing compounds. The recovery (recycling) of arsenic has low economic importance due to its limited use. For this reason, there is little commercial interest to invest in equipment and technology for the recovery of arsenic and its compounds. In addition, there are safety concerns associated with the storage of arsenic in concentrated form and probably terrible consequences associated with any accident in the place of storage. The dilution of arsenic waste with other waste streams and their subsequent dispersion in the environment can meet the regulatory limits, but definitely does not represent a technical solution for arsenic contamination. Currently, encapsulation of arsenic hazardous waste through solidification/stabilization techniques is considered to be the most attractive solution. During this process, contaminants may be chemically bound or encapsulated into a matrix. Cementitious solidification for land disposal of arsenic waste has been recognized by the US EPA and WHO as the best available technology.[26,27]

The present study deals with the possibility of using granular ferric oxide (GFO) to remove pentavalent arsenic As(V) from aqueous solutions by batch adsorption experiments. The equilibrium data were analyzed so that we can understand the adsorption mechanism. Different equilibrium isotherm and kinetic models were applied to fit the experimental data. The impact of different operating conditions (As(V) initial concentration, adsorbent dose, agitation speed, pH, temperature, and presence of phosphates and silica) on the adsorption capacity of the GFO was also investigated. In addition, the possibility of regeneration and reuse of the GFO by different desorbing agents was studied. Results obtained from this study are presented and discussed.

Material and methods

Reagents and solutions

All used chemicals were of analytical laboratory grade, purchased from Merck Slovakia Ltd. All reagents and standards were prepared using demin-

eralized water. The As(V) stock solution was prepared by dissolving an accurately weighed amount of sodium arsenate heptahydrate ($Na_2HAsO_4 \cdot 7H_2O$) in demineralized water to achieve a concentration of 1 g L^{-1}. The stock solutions were subsequently diluted to the required concentrations. To adjust the pH of stock solution, 0.1 M NaOH and 0.1 M HCl were used. After the adsorption, concentrated HCl solution (35 % w/w, ρ = 1.17 g cm^{-3}) was added to the collected samples to store them. In the case of different concentrations of phosphates (PO_4^{3-}) in the As(V) samples, a stock solution of 500 mg L^{-1} PO_4^{3-} was used, which was prepared by dissolving an accurately weighed amount of dipotassium phosphate (K_2HPO_4) in demineralized water. In the case of different concentrations of silica (SiO_2) in the As(V) samples, the required silica concentration was obtained by adding the necessary amount of the solid substance, sodium metasilicate (Na_2SiO_3) directly to the As(V) samples. For As(V) desorption tests, 0.1 M solution of sodium hydroxide (NaOH), hydrochloric acid (HCl), acetic acid (CH_3COOH), sodium chloride (NaCl) and demineralized water were used as desorbing agents.

Instruments and apparatus

The shaking in batch experiments was conducted in a time- and RPM-controlled orbital shaker RSLAB-7PRO (Kvant Ltd., Slovakia). The pH was measured by a digital pH meter Jenway 3510 (Cole-Parmer, United Kingdom) with an accuracy of ± 0.003 unit. A high precision electrical balance ABS 220-4 (Kern & Sohn GmbH, Germany) was used for weighing. For experiments with different temperatures, a refrigerated/heating circulator F12-ED (Julabo, Germany) was used. The adsorption materials were dried in laboratory oven Venticell (MMM Medcenter GmbH, Germany). A PC-controlled automatic electrochemical laboratory analyzer Eca-Flow Model 150 GLP (Istran Ltd., Slovakia) was used for quantitative determination of arsenic in solution.

Analytical determination

Determination of As(V) was done by flow-through chronopotentiometry using triple-electrode flow-through measuring cell (type 353c) with work electrode (type E-T/Au), platinum auxiliary electrode and argentochloride reference electrode. Each sample was analyzed ten times, and calibration was carried out before analysis with a freshly prepared arsenic standard.[28]

Preparation and characterization of adsorbent

A granular ferric oxide (GFO) (Fig. 1) was obtained from Severn Trent (United Kingdom) and was used without further purification. It was only rinsed with demineralized water to remove dirt and then oven-dried at 105 °C for 24 h. Finally, the dried GFO was stored in desiccator for future use. The physicochemical properties of the GFO are shown in Table 1.

Fig. 1 – *Granular ferric oxide*[29]

Table 1 – *Physicochemical properties of GFO*[29]

Parameter	Value
Chemical composition	>70 % Fe_2O_3
Colour	Amber-brown
Bulk density	0.45 g cm^{-3}
Specific surface area	200 m^2 g^{-1}
Particle size	0.5–2.0 mm
Particle porosity	85 %
Applicable for water pH range	6.0–8.0

Adsorption and kinetic studies

Adsorption experiments were carried out by batch method at room temperature (20±2 °C). The 0.1 L of As(V) solution was taken in each Erlenmeyer flask of volume 0.2 L separately, which were placed in the orbital shaker, set at a speed of 150 rpm. The initial concentration of As(V) solution was kept at 1000 μg L^{-1}, while the dose of GFO adsorbent was 0.2 g. The time-dependent behaviour of As(V) adsorption was studied by varying the contact time between the adsorbate and adsorbent in the range 0–180 min (0, 3, 6, 15, 30, 60, 90, 120, 150 and 180 min). The pH of As(V) solution was adjusted to neutral with 0.1 M HCl or 0.1 M NaOH. At the end of each adsorption experiment, the solution and solid phase were separated by filtration with a standard filter paper. The filtrate was collected and subjected for As(V) determination following analytical method. The As(V) concentrations before and after adsorption were recorded, and then the adsorption capacity of GFO and the adsorption (removal) efficiency were calculated by the following equations:

$$q_t = \frac{(c_0 - c_t)V}{m} \quad (1)$$

$$E_a = \frac{(c_0 - c_t)}{c_0} \cdot 100\ \% \quad (2)$$

where q_t is the adsorption capacity (μg g^{-1}) of GFO, E_a is the adsorption (removal) efficiency (%), c_0 and c_t are the initial and final concentration of As(V) in a determined time (μg L^{-1}), V is the volume of As(V) solution (L), and m is the mass of the adsorbent (g). The adsorption equilibrium time of GFO was also determined by this experiment. When the adsorption equilibrium contact time was found, the equilibrium sorption of As(V) onto GFO was carried out by batch method using 0.2 g of GFO and 0.1 L of As(V) solution with various concentrations in range 0–1000 μg L^{-1} (0, 100, 200, 400, 600, 800 and 1000 μg L^{-1}). For this experiment, 0.2 L Erlenmeyer flasks were used on orbital shaker, set at a speed of 150 rpm. The filtrate was collected and subjected to arsenic equilibrium concentration determination. For each As(V) equilibrium concentration, the equilibrium adsorption capacity was calculated according to the following equation:

$$q_e = \frac{(c_0 - c_e)V}{m} \quad (3)$$

where q_e is the equilibrium adsorption capacity (μg g^{-1}), c_0 and c_e is the initial and equilibrium concentration of As(V) (μg L^{-1}), V is the volume of As(V) solution (L), and m is the mass of the adsorbent (g). Then the adsorption data were analyzed to see whether the isotherm obeyed the Langmuir, Freundlich, Redlich-Peterson, Sips or Dubinin-Radushkevich isotherm model equations (Table 3).[30–34] Kinetic parameters were evaluated by pseudo-first and pseudo-second order kinetic model (Table 4).[35–37]

Impact of different operating conditions

The impact of different operating parameters, such as As(V) initial concentration, adsorbent dose, agitation speed, pH, temperature and presence of phosphates and silica, was studied by batch adsorption experiments. The duration of experiments was the adsorption equilibrium time. Thus, As(V) adsorption tests were performed for five different values of each parameter, which are summarized in Table 2. For all operating conditions, if the As(V) concentration was known, adsorption efficiency and capacity was calculated according to Equations 1 and 2.

Desorption experiments

Repeated adsorption-desorption cycles were carried out to study the reversibility of the process and the possibility of GFO material regeneration and reuse in more than one adsorption process. In desorption experiments, 0.2 g of the GFO was firstly exposed to 1000 μg L^{-1} of As(V) solution for the equilibrium time at neutral pH, room temperature (20±2 °C), and agitation speed of 150 rpm. The adsorbent was then separated from the As(V) solution by filtration. The obtained As(V)-loaded adsorbent was then brought in contact with 0.1 L of 0.1 M hydrochloric acid (HCl), 0.1 M acetic acid (CH_3COOH), 0.1 M sodium hydroxide (NaOH), 0.1 M sodium chloride (NaCl), and demineralized water for 2 h in orbital shaker at 150 rpm. Finally, the adsorbent was filtered with a standard filter paper and As(V) content in the filtrate was determined. The adsorption and desorption efficiencies were calculated according to the following equations:

$$E_a = \frac{(c_0 - c_e)}{c_0} \cdot 100\ \% \quad (4)$$

Table 2 – *Experimental setup for study of the impact of different operating conditions*

Changed operating parameter	Stable operating parameter
As(V) initial concentration: 500, 1000, 1500, 2000 and 2500 μg L^{-1}	Volume of solution 0.1 L, contact time 120 min, amount of adsorbent 0.2 g, neutral pH, temperature 20±2 °C, agitation speed 150 rpm
Adsorbent dose: 0.1, 0.2, 0.5, 0.8 and 1.0 g	As(V) initial concentration 1000 μg L^{-1}, volume of solution 0.1 L, contact time 120 min, neutral pH, temperature 20±2 °C, agitation speed 150 rpm
Agitation speed: 100, 150, 200, 250 and 300 rpm	As(V) initial concentration 1000 μg L^{-1}, volume of solution 0.1 L, contact time 120 min, amount of adsorbent 0.2 g, neutral pH, temperature 20±2 °C
pH: 2.5, 4.0, 7.0, 9.0 and 10.5	As(V) initial concentration 1000 μg L^{-1}, volume of solution 0.1 L, contact time 120 min, amount of adsorbent 0.2 g, temperature 20±2 °C, agitation speed 150 rpm
Temperature: 10, 20, 30, 40 and 50 ºC	As(V) initial concentration 1000 μg L^{-1}, volume of solution 0.1 L, contact time 120 min, amount of adsorbent 0.2 g, neutral pH, agitation speed 200 rpm
Presence of phosphates: 0, 1, 2, 3 and 4 mg L^{-1}	As(V) initial concentration 1000 μg L^{-1}, volume of solution 0.1 L, contact time 120 min, amount of adsorbent 0.2 g, neutral pH, temperature 20±2 °C, agitation speed 150 rpm
Presence of silica: 0, 10, 20, 30 and 40 mg L^{-1}	As(V) initial concentration 1000 μg L^{-1}, volume of solution 0.1 L, contact time 120 min, amount of adsorbent 0.2 g, neutral pH, temperature 20±2 °C, agitation speed 150 rpm

$$E_d = \frac{c_d}{c_s} \cdot 100\ \% \tag{5}$$

where E_a is the adsorption efficiency (%), E_d is the desorption efficiency (%), c_0 is the initial concentration of As(V) (μg L^{-1}), c_e is the equilibrium concentration of As(V) (μg L^{-1}), c_d is the As(V) concentration in the solution after desorption (μg L^{-1}), and c_s is the As(V) concentration present on the surface of the adsorbent material after the corresponding previous adsorption (μg L^{-1}).

Experimental data processing

For the experimental data analysis and fitting of the experimental values, nonlinear regression was used. Parameter values of adsorption isotherms, pseudo-first order and pseudo-second order kinetic models were determined by the grid search optimization procedure. The correlation coefficient between the experimental and calculated data was used for the evaluation of the quality of mathematical description of the experimental data:

$$R_{xy} = 1 - \frac{(n-m)S_R^2}{(n-1)S_y^2} \tag{6}$$

where R_{xy} is the correlation coefficient (–), n is the number of measurements, m is the number of parameters, S_R^2 is the residual sum of squares of experimental and calculated values, and S_y^2 is the dispersion of dependent variable values:

$$S_R^2 = \frac{\sum (y_{i,e} - y_{i,c})^2}{n-m} \tag{7}$$

$$S_y^2 = \frac{n\sum y_{i,e}^{\ 2} - \left(\sum y_{i,e}\right)^2}{n(n-1)} \tag{8}$$

where $y_{i,e}$ expresses experimentally measured dependent variable values, $y_{i,c}$ expresses calculated dependent variable values, n is the number of measurements, and m is the number of parameters.

Results and discussion

Modelling of the adsorption

The impact of contact time on adsorption of As(V) on GFO with different time intervals (0−180 min) at initial arsenic concentration 1000 μg L^{-1} and 0.2 g of adsorbent dose is shown in Fig. 2.

As seen in Fig. 2, the adsorption capacity q_t and adsorption (removal) efficiency E_a of GFO rapidly increased in the first 15 minutes, and then continued to increase significantly up to 60 minutes. The fast adsorption rate at the beginning can be explained by the abundant availability of active sites on the adsorbent surface. Finally, the adsorption capacity increased at a lower rate up to 180 minutes and reached 493.0 μg g^{-1}, meaning an adsorption (removal) efficiency equal to 98.60 %.

As the contact time increased, the value of the adsorption capacity and adsorption (removal) efficiency also increased and stabilized at a certain value. There was a balance between adsorbent and adsorbate. From Fig. 2, it was observed that the equilibrium for As(V) adsorption onto GFO was achieved in 120 minutes. Thereafter, the change in adsorption capacity and adsorption (removal) efficiency was negligible. In the equilibrium contact time, the adsorption capacity and adsorption (removal) efficiency of GFO were determined at 449.5 μg g^{-1} and 89.90 %.

In the present study, the Langmuir, Freundlich, Dubinin-Radushkevich, Redlich-Peterson and Sips nonlinear models were used to describe the equilibrium isotherm of As(V) adsorption onto GFO. The summarized isotherm models are shown in Table 3. Fig. 3 describes the modeled isotherm profiles for the adsorption of As(V). For each adsorption model, the correlation coefficient R_{xy} was calculated. Table 3 shows that the Sips and Redlich-Peterson iso-

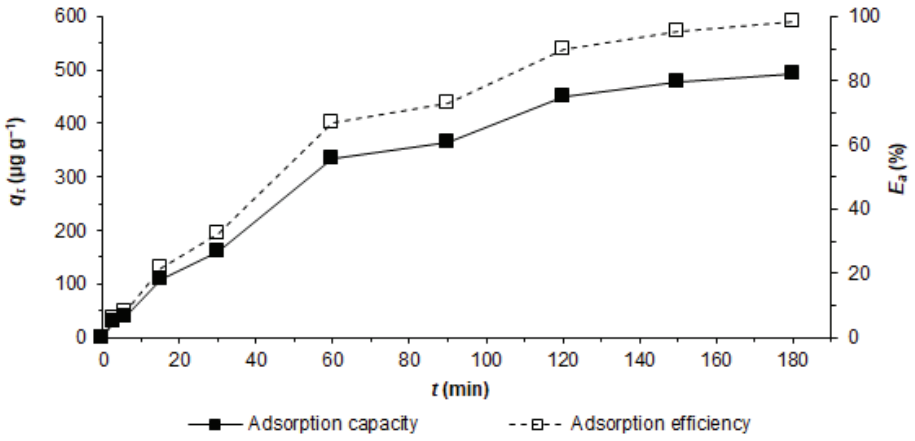

Fig. 2 – *Impact of contact time on the adsorption capacity and adsorption efficiency of GFO for As(V) (As(V) initial concentration 1000 μg L^{-1}, volume of solution 0.1 L, contact time 180 min, amount of adsorbent 0.2 g, neutral pH, temperature 20±2 °C, agitation speed 150 rpm)*

Table 3 – *Isotherm data for adsorption of As(V) onto GFO (As(V) concentration 0–1000 μg L^{-1}, volume of solution 0.1 L, contact time 120 min, amount of adsorbent 0.2 g, neutral pH, temperature 20±2 °C, agitation speed 150 rpm)*

Adsorption isotherm	Equation	Parameter (unit)	Value	R_{xy} (–)
Langmuir (LI)	$q_e = \frac{q_{max} K_L c_e}{1 + K_L c_e}$	q_{max} (μg g^{-1})	1900.00	0.9400
		K_L (L μg^{-1})	6.18·10^{-3}	
	$R_L = \frac{1}{(1 + K_L c_0)}$	R_L (–)	0.10–1.00	
Freundlich (FI)	$q_e = K_F c_e^{1/n}$	K_F (μg$^{(1-1/n)}$ g^{-1} L$^{1/n}$)	20.80	0.9300
		n (–)	1.27	
Dubinin-Radushkevich (D-RI)	$q_e = q_{max} e^{-\beta\varepsilon^2}$	q_{max} (μg g^{-1})	794.00	0.8576
	$\varepsilon = RT\ln(1 + \frac{1}{c_e})$	β (mol^2 kJ^2)	1.83·10^{-4}	
	$E_V = \frac{1}{(2\beta)^{1/2}}$	E_V (kJ mol^{-1})	0.05	
Redlich-Peterson (R-PI)	$q_e = \frac{K_{RP} c_e}{1 + a c_e^b}$	K_{RP} (L g^{-1})	40.96	0.9556
		a (L μg^{-1})^b	3.27	
		b (–)	5.10·10^{-14}	
Sips (SI)	$q_e = \frac{K_S c_e^{\beta_s}}{1 + a_S c_e^{\beta_s}}$	K_S (μg$^{(1-\beta_s)}$ L$^{\beta_s}$ g^{-1})	6.99	0.9602
		a_S (L μg^{-1})$^{\beta_s}$	1.13	
		β_S (–)	9.10·10^{-16}	

where q_e is the equilibrium adsorption capacity; c_e is the equilibrium concentration of adsorbate; c_0 is the initial adsorbate concentration; q_{max} is the maximum theoretical adsorption capacity; K_L, K_F, K_{RP}, K_S, a, b and a_S are different adsorption empirical constants; R_L is the separation factor; ε is the Polanyi adsorption potential; R is the universal gas constant (8.314·10^{-3} kJ mol^{-1} K^{-1}); T is the thermodynamic temperature; β is a constant related to the mean free energy E_V of adsorption per mole of the adsorbate, and β_S is the isothermal exponent.

therm gave the best fit to the experimental equilibrium data for As(V) adsorption according to the values of R_{xy}. These two adsorption isotherms combine the Langmuir and Freundlich isotherm, as well as the heterogeneity of the adsorbent surface and a number of adsorption sites with the same adsorption potential. They describe adsorption on homogeneous and also heterogeneous surfaces. The Langmuir isotherm is valid for monolayer adsorption on the surface that contains a finite number of identical sites where adsorption of only one molecule is possible. This model assumes a uniform surface adsorption energy and no interactions between adsorbed molecules. From this isotherm the Langmuir maximum theoretical adsorption capacity q_{max} can be investigated, which for GFO is equal to 1900.0 μg g^{-1}. The properties of this adsorption can be affirmed from viewpoint of equilibrium parameter R_L, which values were found to be greater than zero and less than one for all initial As(V) concentrations, indicating the favourable adsorption of As(V) by GFO. The Freundlich isotherm is used to describe adsorption characteristics for a heterogeneous surface. The value $1/n$ of Freundlich isotherm lies between zero and one, and it indicates also a favourable sorption process. The Dubinin-Radushkevich isotherm is generally applied to express the adsorption mechanism by Gaussian energy distribution on a heterogeneous surface. Based on the nonlinear plot obtained from Dubinin-Radushkevich model, the value of the adsorption energy E_V was found to be 0.052 kJ mol^{-1}. This value is less than 8 kJ mol^{-1}, indicating that the physical adsorption was the process involved for adsorption of As(V) by GFO. It means that the adsorbed molecules of As(V) could form multilayer adsorption. Based on the results obtained from the isotherm models it follows that the adsorption of As(V) was most probably on heterogeneous surface, favourable, physical and multilayer process.[30–34]

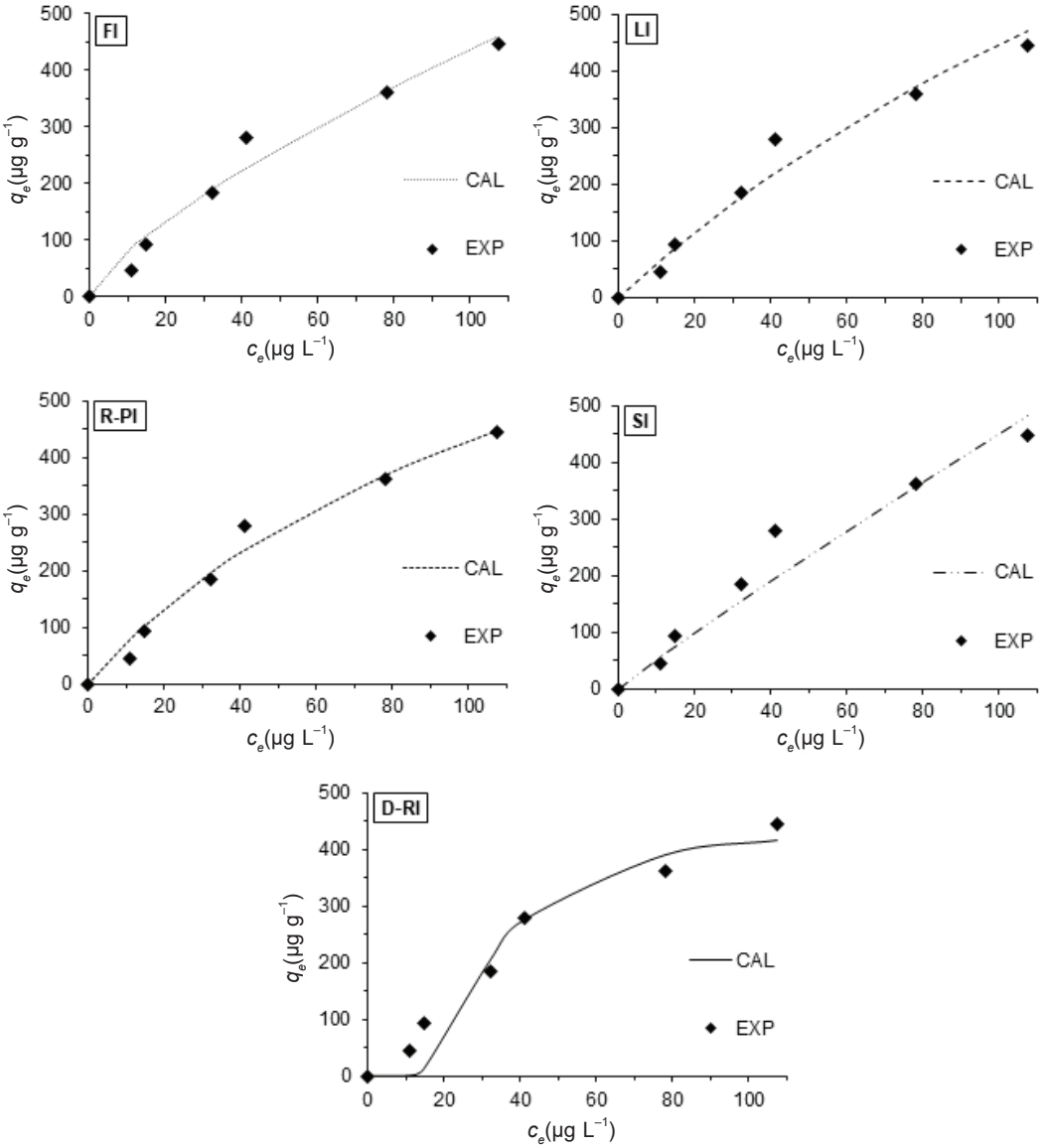

Fig. 3 – *Modelled isotherm profiles of the adsorption of As(V) onto GFO (CAL – calculated values, EXP – experimental values) (As(V) concentration 0–1000 μg L^{-1}, volume of solution 0.1 L, contact time 120 min, amount of adsorbent 0.2 g, neutral pH, temperature 20±2 °C, agitation speed 150 rpm)*

Kinetic studies

Analysis of the kinetic data in the adsorption process is important for describing the adsorption rate, which affects the total time required to form bonds between the adsorbent and the adsorbate. The kinetic parameters obtained from the nonlinear fittings of pseudo-first order (PFO) and pseudo-second order (PSO) models are shown in Table 4. The PFO and PSO plots of kinetic study are illustrated in Fig. 4. Table 4 suggests that the As(V) adsorption onto GFO followed the PFO model with correlation coefficient R_{xy} equal to 0.9901, which assumes that the adsorption sites occupancy rate is proportional to the number of vacant sites.[35–37] The equilibrium adsorption capacity q_e calculated from the PFO kinetic model agree well with the experimental data value equal to 449.5 μg g^{-1}.

Table 4 – *Comparison of PFO and PSO models parameters for As(V) adsorption onto GFO (As(V) initial concentration 1000 μg L^{-1}, volume of solution 0.1 L, contact time 180 min, amount of adsorbent 0.2 g, neutral pH, temperature 20±2 °C, agitation speed 150 rpm)*

Kinetic model	Equation	Parameter (unit)	Value	R_{xy} (–)
PFO	$q_t = q_e\left(1-e^{-k_1 t}\right)$	q_e (μg g^{-1})	500.50	0.9901
		k_1 (min^{-1})	$1.65\cdot10^{-2}$	
PSO	$q_t = \frac{k_2 q_e^2 t}{1+k_2 q_e t}$	q_e (μg g^{-1})	520.00	0.9261
		k_2 (g μg^{-1} min^{-1})	$5.16\cdot10^{-5}$	

where q_t is the adsorption capacity in time t, q_e is the equilibrium adsorption capacity, k_1 is the pseudo-first order rate constant, and k_2 is the pseudo-second order rate constant.

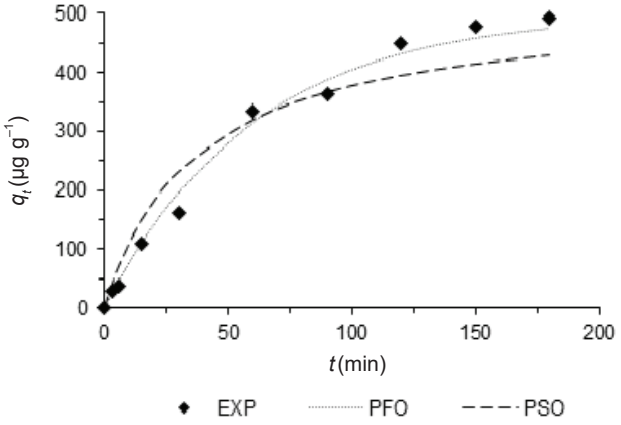

Fig. 4 – *Modelled PFO and PSO kinetic profiles of the adsorption of As(V) onto GFO (As(V) initial concentration 1000 μg L^{-1}, volume of solution 0.1 L, contact time 180 min, amount of adsorbent 0.2 g, neutral pH, temperature 20±2 °C, agitation speed 150 rpm)*

Impact of different operating conditions

It is important to understand the impact of different operating conditions on As(V) adsorption by GFO media, since the treatment economics can be significantly affected. The impact of each operating parameter on As(V) adsorption by GFO is illustrated in Fig. 5. The impact of initial As(V) concentration was studied in range from 500 to 2500 μg L^{-1}. The adsorption (removal) efficiency E_a decreased (from 95.02 % to 71.38 %) with the increase in As(V) initial concentration. The lower efficiencies for higher concentrations can be explained by the saturation of active adsorption sites, which caused decrease in the amount of available sites for further adsorption. On the other hand, naturally, the adsorption capacity q_t of GFO increased with the increase in initial concentration of As(V).

The different doses of GFO used were 0.1, 0.2, 0.5, 0.8, and 1 g. The adsorption (removal) efficiency E_a increased with the increasing adsorbent material doses until almost 100 %. It is logical that more material means more available free sites for adsorption. From the adsorbent dose of 0.5 g, there was no remarkable increase in the adsorption (removal) efficiency. The optimum dose was 0.5 g of GFO, reaching 98.63 % efficiency.

From the study of different agitation speeds, from 100 to 300 rpm, it was obtained that the adsorption (removal) efficiency E_a increased with the agitation speed. This could have been due to the fact that the external mass transfer effect increased with the increase in agitation, resulting in better transport of solute from solution to the adsorbent active sites, and thus increasing the rate of adsorption. Maximum removal was observed at 250 rpm with adsorption (removal) efficiency of 98.73 %. However, at agitation speeds of 200, 250 and 300 rpm, the aqueous solutions were mixed so intensively that the turbulence caused more frequent abrasion of the adsorbent particles, and turbidity was observed in the aqueous solution.

In general, As(V) adsorption (removal) efficiency E_a decreased with increasing pH. Then, it increased at pH 9.0, but with further increase in pH, it rapidly decreased. The maximum adsorption (removal) efficiency (99.00 %) was reached in acidic conditions, at pH 2.5. However, due to this pH, the adsorbent material was partially destroyed and part of the iron contained in the material was dissolved in the solution. Acidic condition is not recommended and optimum pH was found to be between 6.5 and 8.0, which is the most common pH range for ground or surface sources of drinking water.

The impact of temperature was investigated at different values like 10, 20, 30, 40 and 50 ºC. From 10 to 30 ºC the adsorption (removal) efficiency E_a generally increased, reaching the highest level at 30 ºC (97.55 %), and then at 50 ºC the efficiency decreased to 73.08 %.

Generally, adsorption (removal) efficiency E_a of the adsorbent decreased with increasing phosphates and silica concentration in the sample. It is known that phosphate ions are very adsorptive on the surface of ferric oxides (Fe_2O_3) present in GFO.[38] Results indicate that arsenates and phosphates competed for the same surface sites. In the silica case, it is assumed that silica can increase the electrostatic repulsion of As(V), and can also reduce the number of available sites for the As(V) adsorption by coating the surface of GFO.[39]

Desorption – regeneration of GFO

The reversibility of As(V) sorption onto GFO was studied using acidic (0.1 M HCl and 0.1 M CH_3COOH), basic (0.1 M NaOH), neutral (0.1 M NaCl) extracting solutions and demineralized water (Demi H_2O). Three cycles of adsorption and desorption were performed. The results are presented in Fig. 6. It is evident that the desorption efficiency E_d depended on the nature of the desorbing solution. Both acid desorbing agents caused structural damage to the adsorbent material, which was destroyed and dissolved giving to the solution a yellow-orange colour and turbidity. In the case of 0.1 M HCl, the As(V) determination was not possible in the samples. The acid desorbing agents were not suitable for GFO regeneration. The basic solution of 0.1 M NaOH achieved the highest desorption efficiency along the three desorption processes, being 78.47 % for the first desorption, 74.19 % for the second, and 45.82 % for the third. Therefore, this solution was suitable for repeated regeneration of the tested GFO adsorbent. However, after the sec-

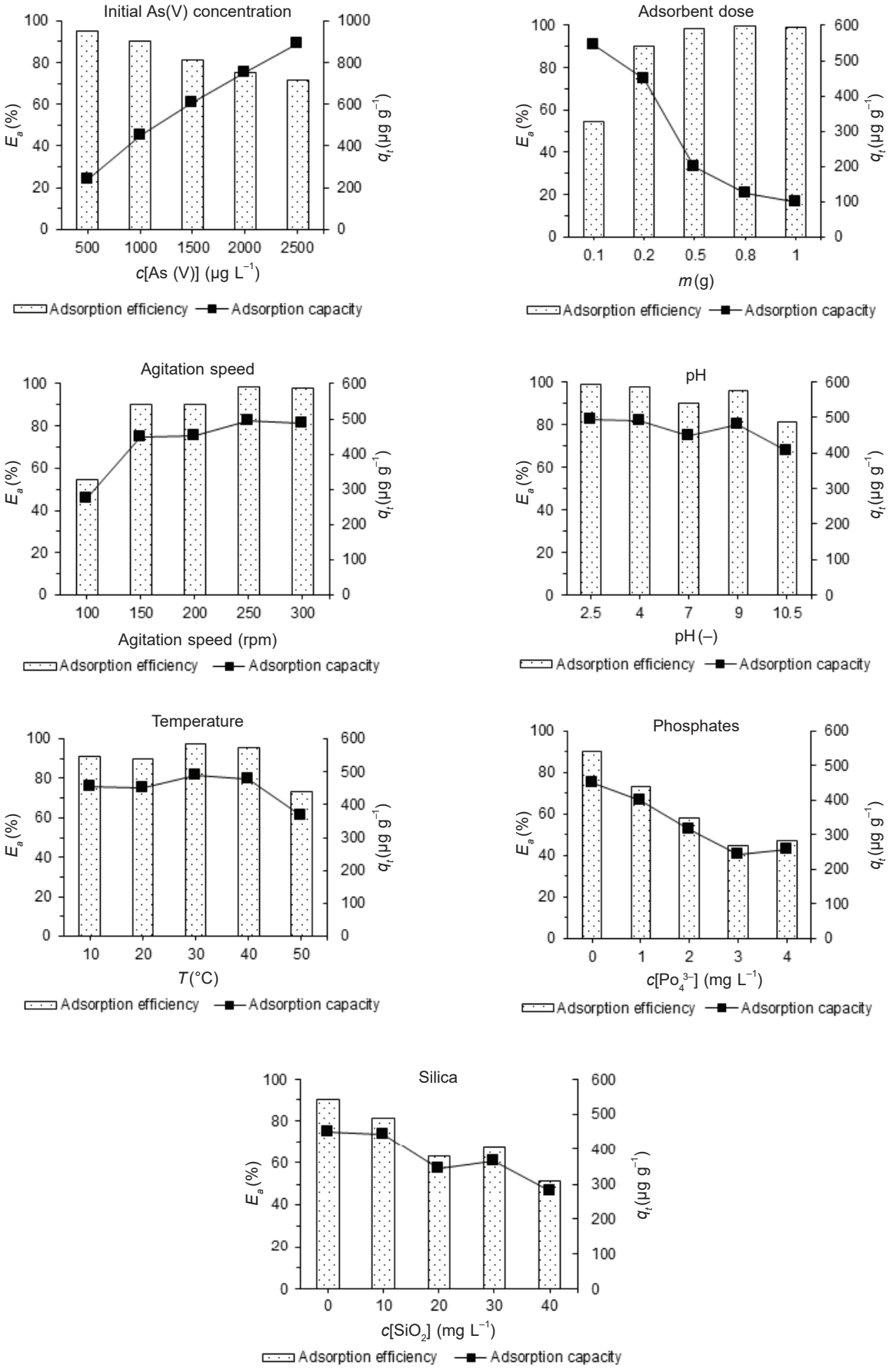

Fig. 5 – *Impact of different operating conditions on As(V) adsorption by GFO*

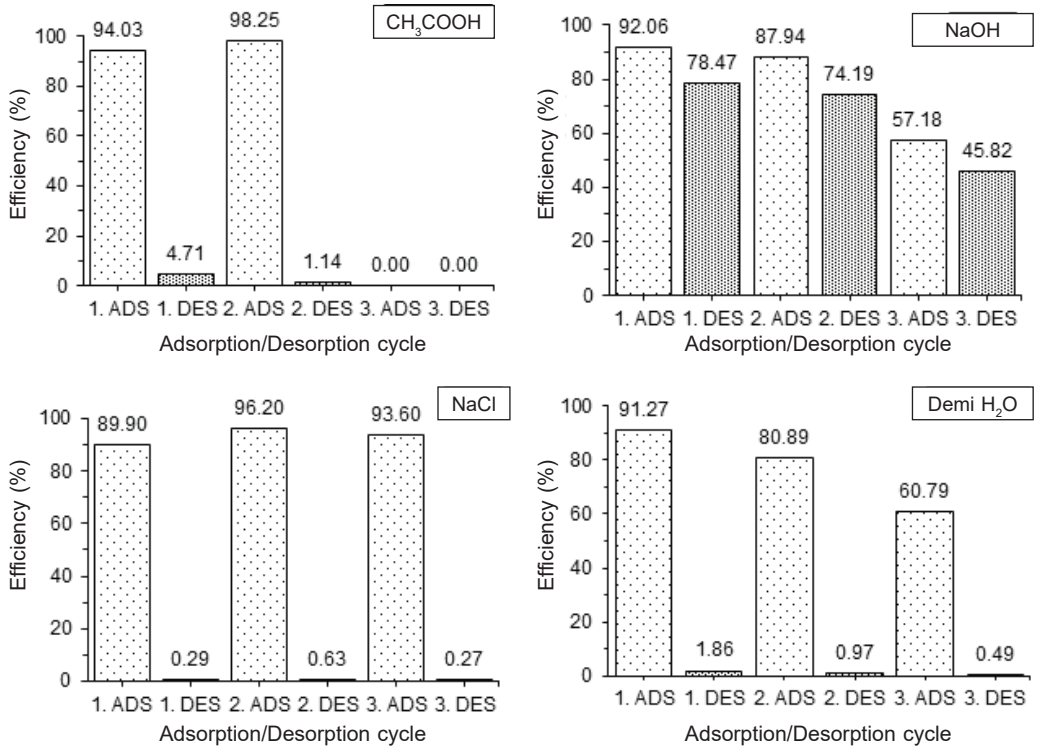

Fig. 6 – *Histograms showing the efficiency of adsorption and desorption of As(V) using various desorbing agents (As(V) initial concentration 1000 μg L^{-1}, volume of solution 0.1 L, contact time 120 min, amount of adsorbent 0.2 g, neutral pH, temperature 20±2 °C, agitation speed 150 rpm)*

ond cycle, adsorption and desorption efficiency decreased, probably because of structural damage of the adsorbent material by the basic solution. Finally, under neutral conditions, using demineralized water and 0.1 M NaCl, the desorption efficiency was practically insignificant, but adsorption efficiency was kept high during the regeneration cycles. Maybe these two desorbing agents did not cause structural damage to GFO, and additionally the saturation of GFO was not achieved. Based on the results obtained from the experiments with demineralized water, it can be stated that the adsorption of As(V) onto the GFO was strong, and As(V) was not desorbed back into the demineralized water.

Conclusions

The present study shows that the GFO was successfully used as an adsorbent for the quantitative removal of As(V) from aqueous solutions. The applied mathematical models provided reasonable predictive performance of As(V) adsorption and worked satisfactorily. Based on the results obtained from the equilibrium and kinetic models, it follows that the adsorption of the As(V) onto GFO was favourable, physical and multilayer process. The study on equilibrium adsorption revealed that the Redlich-Peterson and Sips isotherm model (R_{xy} > 0.95) and pseudo-first order kinetic model (R_{xy} > 0.99) gave the best fit to experimental data. Under the equilibrium conditions, the maximum theoretical adsorption capacity of GFO predicted by the model was 1 900 μg g^{-1}. According to the results obtained from the impact of different operating conditions on As(V) removal from aqueous solutions, it follows that the adsorption (removal) efficiency decreased with the increase in As(V) initial concentration, and also with increased phosphates and silica concentration, the optimum dose of GFO was found to be 0.5 g, and the optimum pH was found between 6.5 and 8.0, the maximum As(V) removal was observed at agitation speed of 250 rpm and temperature of 30 ºC. The basic solution of 0.1 M NaOH was suitable for repeated regeneration of the tested GFO, which caused the highest desorption efficiencies (78.47 %, 74.19 %, and 45.82 %) along the three adsorption-desorption cycles. Finally, it can be concluded that the application of static experiments is an effective method for modelling, optimization, and design of the adsorption process for As(V) removal from aqueous solutions.

ACKNOWLEDGEMENT

The authors would like to thank for financial contribution from the Slovak University of Technology Grant scheme for Support of Excellent Teams of Young Researchers.

References

1. URL: https://ec.europa.eu/environment/water/water-drink/review_en.html (30.8.2021.)
2. *Sadiya, A., Shafinaz, S., Norahim, I., Mohammed, J. N., Dai-Viet, N. V., Fazilah, A. M.,* Arsenic removal technologies and future trends: A mini review, J. Clean. Prod. **278** (2021) 1. doi: https://doi.org/10.1016/j.jclepro.2020.123805
3. *Singh, R., Singh, S., Parihar, P., Singh, V. P., Prasad, S. M.,* Arsenic contamination, consequences and remediation techniques: A review, Ecotoxicol. Environ. Saf. **12** (2015) 247. doi: https://doi.org/10.1016/j.ecoenv.2014.10.009
4. *Wang, S., Mulligan, C. N.,* Occurrence of arsenic contamination in Canada: Sources, behavior and distribution, Sci. Total Environ. **366** (2006) 701. doi: https://doi.org/10.1016/j.scitotenv.2005.09.005
5. *Huq, M. E., Fahad, S., Shao, Z., Sarven, M. S., Khan, I. A., Alam, M., Saeed, M., Ullah, H., Adnan, M., Saud, S., Cheng, Q., Ali, S., Wahid, F., Zamin, M., Raza, M. A., Saeed, B., Riaz, M., Khan, W. U.,* Arsenic in a groundwater environment in Bangladesh: Occurrence and mobilization, J. Environ. Manage. **262** (2020) 110318. doi: https://doi.org/10.1016/j.jenvman.2020.110318
6. *Shakya, A. K., Ghosh, P. K.,* Simultaneous removal of arsenic and nitrate in absence of iron in an attached growth bioreactor to meet drinking water standards: Importance of sulphate and empty bed contact time, J. Clean. Prod. **186** (2018) 304. doi: https://doi.org/10.1016/j.jclepro.2018.03.139
7. *Smedley, P. L., Kinniburgh, D. G.,* A review of the source, behavior and distribution of arsenic in natural waters, J. Appl. Geochem. **17** (2001) 517. doi: https://doi.org/10.1016/S0883-2927(02)00018-5
8. *Katsoyiannis, I. A., Zouboulis, A. I.,* Application of biological processes for the removal of arsenic from groundwaters, Water Res. **38** (2004) 17. doi: https://doi.org/10.1016/j.watres.2003.09.011
9. *Hung, D. Q., Nekrassova, O., Compton, R. G.,* Analytical method for inorganic arsenic in water: Review, Talanta **64** (2004) 269. doi: https://doi.org/10.1016/j.talanta.2004.01.027
10. *Pal, P.,* Groundwater Arsenic Remediation: Treatment Technology and Scale Up, Elsevier, Oxford, 2015, 326.
11. *Luong, V. T., Kurz, E. E. C., Hellriegel, U., Luu, T. L., Hoinkis, J., Bundschuh, J.,* Iron-based subsurface arsenic removal technologies by aeration: A review of the current state and future prospects, Water Res. **133** (2018) 110. doi: https://doi.org/10.1016/j.watres.2018.01.007
12. *Weerasundara, L., Ok, Y. S., Bundschuh, J.,* Selective removal of arsenic in water: A critical review, Environ. Pollut. **268** (2021) 1. doi: https://doi.org/10.1016/j.envpol.2020.115668
13. *Ungureanu, G., Santos, S., Boaventura, R., Botelho, C.,* Arsenic and antimony in water and wastewater: Overview of removal techniques with special reference to latest advances in adsorption, J. Environ. Manage. **151** (2015) 326. doi: https://doi.org/10.1016/j.jenvman.2014.12.051
14. *Chen, H., Zhao. T., Sun, D., Wu, M., Zhang, Z.,* Changes of RNA N6-methyladenosine in the hormesis effect induced by arsenite on human keratinocyte cells, Toxicology in Vitro **56** (2019) 84. doi: https://doi.org/10.1016/j.tiv.2019.01.010
15. *Karim, M. D. M.,* Arsenic in groundwater and health problems in Bangladesh, Water Res. **34** (2000) 304. doi: https://doi.org/10.1016/S0043-1354(99)00128-1
16. *Nurchi, V. M., Djordjevic, A. B., Crisponi, G., Alexander, J., Bjørklund, G., Aaseth, J.,* Arsenic toxicity: molecular targets and therapeutic agents, Biomolecules **10** (2020) 1. doi: https://doi.org/10.3390/biom10020235
17. URL: https://www.who.int/water_sanitation_health/water-quality/guidelines/chemicals/arsenic.pdf (30.8.2021.)
18. *Choong, T. S. Y., Chuah, T. G., Robiah, Y., Koay, F. L. G., Azni, I.,* Arsenic toxicity, health hazards and removal techniques from water: An overview, Desalination **217** (2007) 139. doi: https://doi.org/10.1016/j.desal.2007.01.015
19. *Baig, S. A., Sheng, T., Hu, Y., Xu, J., Xu, X.,* Arsenic removal from natural water using low cost granulated adsorbents: A review, Clean – Soil Air Water **43** (2015) 13. doi: https://doi.org/10.1002/clen.201200466
20. *Höll, W. H.,* Mechanisms of arsenic removal from water, Environ Geochem Health **32** (2010) 287. doi: https://doi.org/10.1007/s10653-010-9307-9
21. *Zhu, J., Pigna, M., Cozzolino, V., Caporale, A. G., Violante, A.,* Higher sorption of arsenate versus arsenite on amorphous Al-oxide, effect of ligands, Environ. Chem. Lett. **11** (2013) 289. doi: https://doi.org/10.1007/s10311-013-0405-7
22. *Sarkar, A., Paul, B.,* The global menace of arsenic and its conventional remediation – A critical review, Chemosphere **158** (2016) 37. doi: https://doi.org/10.1016/j.chemosphere.2016.05.043
23. *Mohan, D., Pittman, C. U.,* Arsenic removal from water/wastewater using adsorbents – A critical review, J. Hazard. Mater. **142** (2007) 1. doi: https://doi.org/10.1016/j.jhazmat.2007.01.006
24. *Nguyen, T. V., Loganathan, P., Vigneswaran, S., Krupanidhi, S., Pham, T. T. N., Ngo, H. H.,* Arsenic waste from water treatment systems: Characteristics, treatments and its disposal, Water Sci. Technol. Water Supply **14** (2014) 939. doi: https://doi.org/10.2166/ws.2014.073
25. *Devi, P., Saroha, A. K.,* Utilization of sludge based adsorbents for the removal of various pollutants: A review, Sci. Total Environ. **578** (2017) 16. doi: https://doi.org/10.1016/j.scitotenv.2016.10.220
26. *Leist, M., Casey, R. J., Caridi, D.,* The management of arsenic wastes: Problems and prospects, J. Hazard. Mater. **76** (2000) 125. doi: https://doi.org/10.1016/S0304-3894(00)00188-6
27. *Nguyen, T. V., Loganathan, P., Vigneswaran, S., Krupanidhi, S., Pham, T. T. N., Ngo, H. H.*, Arsenic waste from water treatment systems: Characteristics, treatments and its disposal, Water Sci. Technol. Water Supply **14** (2014) 939. doi: https://doi.org/10.2166/ws.2014.073
28. *Cacho, F., Lauko, L., Manova, A., Dzurov, J., Beinrohr, E.,* Sequential determination of total arsenic and cadmium in concentrated cadmium sulphate solutions by flow-through stripping chronopotentiometry after online cation exchanger separation, J. Anal. Methods Chem. **2012** (2012) 1. doi: https://doi.org/10.1155/2012/814983
29. *Zakhar, R.,* Arsenic removal from water and its impact on selected species of organisms, PhD thesis, Slovak University of Technology in Bratislava, Bratislava, 2020, 192. https://opac.crzp.sk/?fn=detailBiblioForm&sid=8E0A01F-6D74C9FCBC84BEE1E231C (30.8.2021.)
30. *Foo, K. Y., Hameed, B. H.,* Insights into the modeling of adsorption isotherm systems, Chem. Eng. J. **156** (2010) 2. doi: https://doi.org/10.1016/j.cej.2009.09.013
31. *Dada, A. O., Olalekan, A. P., Olatunya, A. M., Dada, O.,* Langmuir, Freundlich, Temkin and Dubinin-Radushkevich isotherms studies of equilibrium sorption of Zn^{2+} unto phosphoric acid modified rice husk, J. Appl. Chem. **3** (2012) 38. doi: https://doi.org/10.9790/5736-0313845

32. *Das, B., Mondal, N. K., Bhaumik, R., Roy, P.,* Insight into adsorption equilibrium, kinetics and thermodynamics of lead onto alluvial soil, Int. J. Environ. Sci. Technol. **11** (2014) 1101.
doi: https://doi.org/10.1007/s13762-013-0279-z
33. *Roy, P., Mondal, N. K., Das, K.,* Modeling of the adsorptive removal of arsenic: A statistical approach, J. Environ. Chem. Eng. **2** (2014) 585.
doi: https://doi.org/10.1016/j.jece.2013.10.014
34. *Ayawei, N., Ebelegi, A. N., Wankasi, D.,* Modelling and interpretation of adsorption isotherms, J. Chem. **2017** (2017) 1.
doi: https://doi.org/10.1155/2017/3039817
35. *Lin, J., Wang, L.,* Comparison between linear and non–linear forms of pseudo-first-order and pseudo-second-order adsorption kinetic models for the removal of methylene blue by activated carbon, Front. Environ. Sci. Eng. **3** (2009) 320.
doi: https://doi.org/10.1007/s11783-009-0030-7
36. *Ryu, S. R., Jeon, E. K., Yang, J. S., Kitae, B.,* Adsorption of As(III) and As(V) in groundwater by Fe-Mn binary oxide-impregnated granular activated carbon (IMIGAC), J. Taiwan Inst. Chem. Eng. **72** (2017) 62.
doi: https://doi.org/10.1016/j.jtice.2017.01.004
37. *Urminská, B., Derco, J., Zakhar, R., Korpicsová, A.,* Use of zeolites for macronutrients removal from wastewater, Acta Chimica Slovaca **12** (2019) 150.
doi: https://doi.org/10.2478/acs-2019-0021
38. *Neupane, G., Donahoe, R. J., Arai*, *Y.*, Kinetics of competitive adsorption/desorption of arsenate and phosphate at the ferrihydrite-water interface, Chem. Geol. **368** (2014) 31.
doi: https://doi.org/10.1016/j.chemgeo.2013.12.020
39. *Möller, T., Sylvester*, *P.*, Effect of silica and pH on arsenic uptake by resin/iron oxide hybrid media, Water Res. **42** (2008) 1760.
doi: https://doi.org/10.1016/j.watres.2007.10.044